Regular Article

PHYSICAL CHEMISTRY RESEARCH
Published by the
Iranian Chemical Society
www.physchemres.org
info@physchemres.org

***Phys. Chem. Res.**, Vol. 5, No. 2, 221-237, June 2017*
DOI: 10.22036/pcr.2017.40619

Molecular Dynamics Simulation of Al/NiO Thermite Reaction Using Reactive Force Field (ReaxFF)

M. Fathollahi[a,*] and H. Azizi Toupkanloo[b]

[a]*Faculty of Material and Manufacturing Technologies, Malek Ashtar University of Technology, P.O. Box: 16765-3454, Tehran, Iran*
[b]*University of Neyshabur, Neyshabur, Iran*

(Received 21 September 2016, Accepted 26 November 2016)

In this work, the thermal reaction of aluminum (Al) and nickel oxide (NiO) was investigated by molecular dynamics simulations. Some effective features of reaction such as reaction temperature, reaction mechanism, and diffusion rate of oxygen into aluminum structure were studied. ReaxFF force field was performed to study the Al/NiO thermite reaction behavior at five different temperatures (500, 900, 1100, 1200 and 1400 K). The results obtained from the molecular dynamics simulation predict that the reaction temperature for aluminum metal and nickel oxide mixture would be 1141 K, which is in a good agreement with that of the experimental value (*i.e.* 1148.8 K). In addition, the mean square displacement analysis suggests that the movement of aluminum atoms is less than that of oxygen and nickel atoms. The estimated diffusion coefficient of oxygen in the aluminum/nickel oxide thermite mixtures was 4.53×10^{-8} m^2 s^{-1}. The results show that the diffusion coefficients significantly increase with increasing temperature.

Keywords: Thermite reaction, Al/NiO system, Molecular dynamics simulation, ReaxFF force field

INTRODUCTION

Energetic materials or reactive materials are assumed as materials with high enthalpies of formation, which can release the chemical energy stored within their molecular structures in a reproducible manner upon stimulus through heat, impact, shock, spark, *etc*., generally with the release of large quantities of hot gaseous products. Reactive materials include three major categories: thermites [1,2], intermetallics [3,4] and metal-polymer mixtures [5]. Among these categories, thermites are of great consideration due to the fact that they are widely used as civilian and military applications needed large and rapid heating, including welding [6,7], alloying [8,9], gas generators [10,11], material synthesis [12,13], micro-heaters (or thrusters, detonators, and initiators) [14-17], igniters [18], and lead free gun primers [19]. In particular, thermite reactions can be described as an exothermic heterogeneous mixture of metal (fuel) and oxidizer particles where a metal powder and a metallic oxide (oxidizer) interact in an oxidation-reduction reaction manner with the evolution of a large amount of heat [20,21].

Goldschmidt [22] introduced the concept of "thermite" in the 1895s while planning to come up with very pure metals. Among various metals such as aluminum, magnesium, titanium, zinc, silicon and boron, aluminum is the most commonly used fuel in thermites due to its high affinity for oxygen, easy handling, high reactivity, the abundance, and high boiling temperature [23]. Many of the metal oxides including Fe_2O_3 [24-26], CuO [27-29], MoO_3 [30,31], WO_3 [32] Bi_2O_3 [33,34], NiO [35-37], *etc.* can be used as a oxidizer in the thermite reactions.

From the experimental perspective, much research has been conducted so far to explore the thermal behavior of thermite reactions [2,24,27,31,33,37]. In the literature, there are very few theoretical studies available as compared with experimental studies aimed at demonstrating the behavioral

*Corresponding author. E-mail: fathollahimanoochehr@gmail.com

parameters of the thermite reactions [3,25]. Using several characterization techniques such as scanning electron microscopy, electro-thermal analysis and differential scanning calorimetry, can be used to obtain knowledge on the thermite reaction including reaction temperature, mechanism of reaction, energy release, and *etc*. [29,38].

Complementing experimental effort on the energetic properties of the thermite reactions, molecular simulations have provided insight into the atomistic mechanisms driving the reaction progress. Nevertheless, computer simulation, especially molecular dynamics (MD) simulation, can provide an efficient method on atomic level to study the various properties of thermite reactions such as migration behavior of oxygen atom and estimate the reaction temperature, without the need of any other experiment apparatus. The choice of a suitable force field is an important factor in the calculations using MD simulations. As bonds are broken and formed in the thermite reaction, the special force field must be chosen. Among different available force fields, the ReaxFF force field for interatomic potentials is a powerful computational tool for exploring, developing, and optimizing thermite material properties [39]. The important advantage of the ReaxFF approach is to model the formation and breaking of bonds through several orders of magnitude which are faster as compared with the traditional quantum mechanical models. There are only few MD investigations conducted using ReaxFF on the thermite reactions. Quite recently, Zhu and coworkers [25] investigated the MD simulation on Al (nanosphere)/Fe_2O_3 (nanotube) thermite reaction using ReaxFF. They measured the variations in chemical bonds to elaborate the reaction process and characterize the ignition performance as well. Furthermore, they found that under the temperature of 1450 K, oxygen is directly released from hematite nanotube, thermite reaction is deemed as a multiphase process. Jin-Ping and coworkers [40] studied the behavior of Al/SiO_2 thermite reaction through MD simulation using ReaxFF. Their results demonstrated that by increasing the initial temperature, the effective reaction time decreases.

To the best of our knowledge, however, the effects of the temperature and oxygen diffusion coefficients estimated for the Al/NiO thermite reaction behavior are not fully understood. In this case, we could refer to the work performed by Wen and coworkers [37].

In this work, the following stoichiometric reaction can be considered:

$$2Al + 3NiO \rightarrow 3Ni + Al_2O_3 \quad (1)$$

In the final phases, Al_2O_3 and Ni components are formed through a situ chemical reaction in which Al reduces the nickel oxidize.

The main focus of the present study is to characterize the MD simulation results such as reaction mechanism involved the formation and breaking of chemical bonds, structure evolution during reaction process, mean square displacement parameter, diffusion coefficient, and radial distribution function analysis for Al/NiO thermites reaction at different temperatures.

Simulation Details

All the calculations for MD simulation of thermal reaction between Al and NiO compounds were performed using LAMMPS software [3,25,40,41]. The conjugate gradient (CG) algorithm were used as molecular dynamics algorithm for either of the energy minimization and the MD steps. The assigned tolerance for energy and force was 6-10 and 4-10, respectively. The 12.5 angstrom was used for van der Waals forces cutoff.

To model the interactions between aluminum and nickel oxide structure, the Reaxff force field and NVE ensemble were used. All simulations were divided into two stages in the canonical ensemble (NVT) with time steps set to 1 fs for all simulation cases.

Step 1: Molecular dynamics relaxation. The NVT-MD simulations on Al/NiO thermite mixture were performed to reach thermal equilibrium after 10 ps. A Nose-Hover thermostat with a temperature-damping constant was used to control the temperature of system [3,25].

Step 2: Reaction simulation. Then, to evaluate thermite reaction characteristics, NVE simulations were carried out for 300 ps.

Reaxff Force Field

The total interaction energy expression of ReaxFF is divided into several energy terms as given in the following Eq. (2) [41].

$$E_{total} = E_{bond} + E_{under} + E_{over} + E_{val} + E_{torsion} + E_{vdWaals} + E_{coulomb} \quad (2)$$

The partial contributions in Eq. (1) consist of bond energies (E_{bond}), energy contributions to penalize overcoordination and (optionally) stabilize under-coordination of atoms (E_{over} and E_{under}), valence angle energies (E_{val}), angle torsion ($E_{torsion}$), terms to handle nonbonded Coulomb ($E_{coulomb}$) and van der Waals ($E_{vdWaals}$) interaction energies. As mentioned above, a fundamental difference between ReaxFF and unreactive force fields is that ReaxFF does not use fixed connectivity assignments for the chemical bonds. Therefore, ReaxFF is based on a bond order/bond distance relationship, a concept developed by Tersoff [42] and first employed to carbon chemistry by Brenner [43]. Momently bond orders (BO_{ij}), including contributions from sigma, π, and π-π bonds are calculated from the interatomic distances using Eq. (3).

$$BO_{ij} = BO_{ij}^{\sigma} + BO_{ij}^{\pi} + BO_{ij}^{\pi\pi} = \exp\left[P_{bol}\left(\frac{r_{ij}}{r_0^{\sigma}}\right)^{P_{bo2}}\right] + \exp\left[P_{bo3}\left(\frac{r_{ij}}{r_0^{\pi}}\right)^{P_{bo4}}\right] + \exp\left[P_{bo5}\left(\frac{r_{ij}}{r_0^{\pi\pi}}\right)^{P_{bo6}}\right] \quad (3)$$

where BO is the bond order between atoms i and j, r_{ij} is interatomic distance, r_o terms are equilibrium bond lengths, and p_{bo} terms are empirical parameters. Particularly, Reaxff force field has been successfully used for a variety of solid structures [44,45]. However, it is worth mentioning that three interaction types need to be taken into account while exploring the thermal reaction for the Al/NiO compound: interaction of NiO atoms with each other, Al atoms with each other, and Al atoms with Ni and O atoms present in the NiO structure. In this way, we attempted to use the reported information from previous studies. For doing so, all the parameters required for Reaxff force field interaction functions were extracted from previous studies in this field, such as Shine *et al.* [46] for the interaction between Al-Ni, Navaro *et al.* [47] for Ni-Ni and Ni-O interaction, and Hong *et al.* [44] for Al-Al and Al-O interaction.

Simulation Box

Simulation box was built on three separate layers; two aluminum layers and one NiO structure layer in between. A schematic of this box can be seen in Fig. 1.

It should be noted that aluminum layer has a distance of 4 Å from NiO layer and the simulation box has dimensions equal to 32.860 × 29.176 × 29.176 $Å^3$. The simulation box involves 764 aluminum, 588 oxygen and 588 nickel atoms.

RESULTS AND DISCUSSION

To examine the accuracy of results, before elaborating the thermal behavior of Al/NiO thermite system, the pure aluminum and nickel oxide structures should be considered separately.

Pure Structures

To investigate the accuracy of the results, we first investigated the structural properties of pure Al and NiO given the obtained output data of Reaxff force field. To do so, two simulation boxes were built; one containing aluminum with dimensions equal to 40.50 × 20.25 × 20.25 $Å^3$ and the other containing nickel oxide with dimensions equal to 62.5 × 20.8 × 20.8 $Å^3$. Afterwards, aluminum and nickel oxide structures reached the structural equilibrium at 300 K and the pressure of 1 atm using MD method under NPT ensemble. In this simulation, the time step was 1 femtosecond (fs) while total simulation time was 100 picosecond (ps).

Whenever the coefficients used in the Reaxff force field are appropriate for the MD simulation, it is possible to fully predict the crystal structure properties of aluminum and nickel oxide at ambient temperature and pressure. Therefore, radial distribution function (RDF) analysis was used for investigating their crystal structure and verifying the accuracy of the simulation results.

The pair correlation function (RDF) diagrams related to Al-Al atoms for the aluminum structure and Ni-O atoms for nickel oxide atoms obtained from simulation were compared with their original structures before simulation, which can be seen in Figs. 2 and 3, respectively. A comparison between the position of first Al-Al peak before and after the simulation at the RDF diagram shows that this peak is located at 2.85 Å without any shift (Fig. 3).

RDF diagram of Ni-O bond for nickel oxide structure before and after simulation is displayed in Fig. 3. As shown

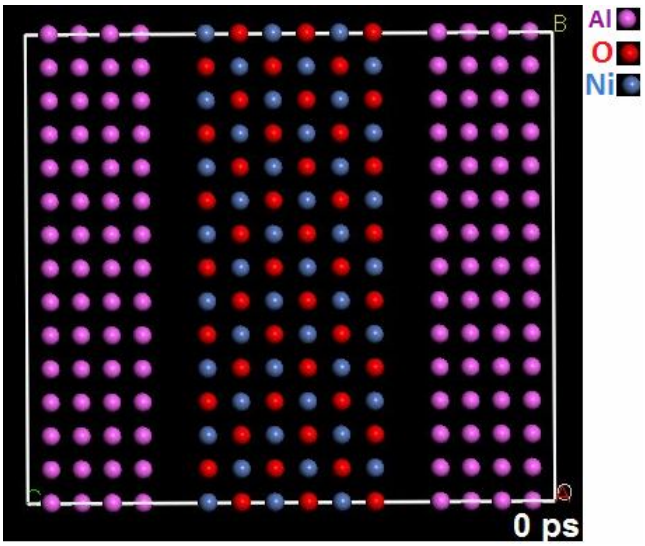

Fig. 1. The initial simulation box.

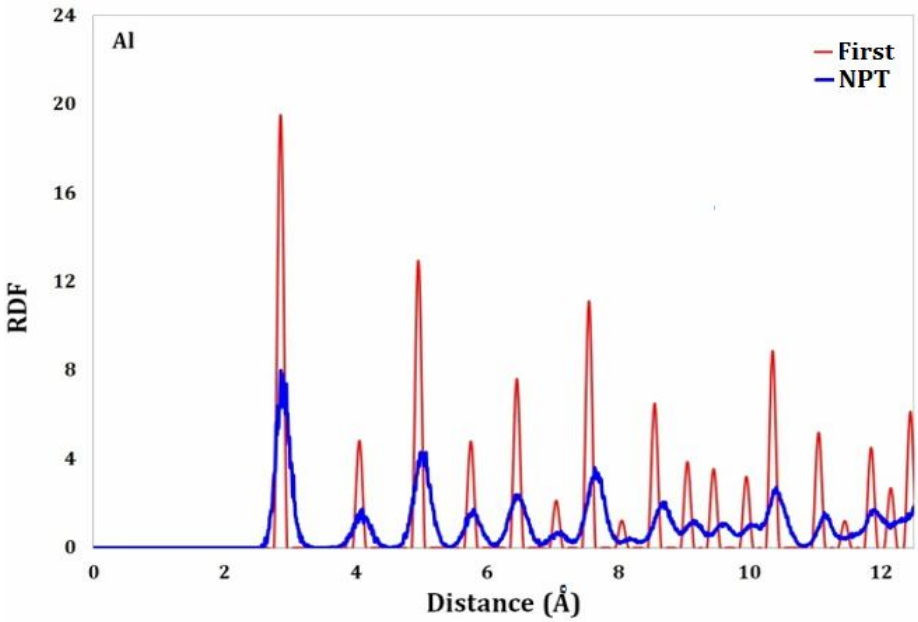

Fig. 2. The pair correlation function calculated for Al-Al before and after simulation.

in this figure, the first characteristic Ni-O peak is located exactly at 2.05 A before and after simulation without any change. This observation indicates that the simulation results show very good agreement for the structural properties of nickel oxide. According to the observed results from RDF diagram, the choice of Reaxff force field is suitable for describing the present thermite system and could correctly reproduce the trend of this system.

For a better view, the charts of Figs. 2 and 3 are smoothed for after simulation process. The present peaks

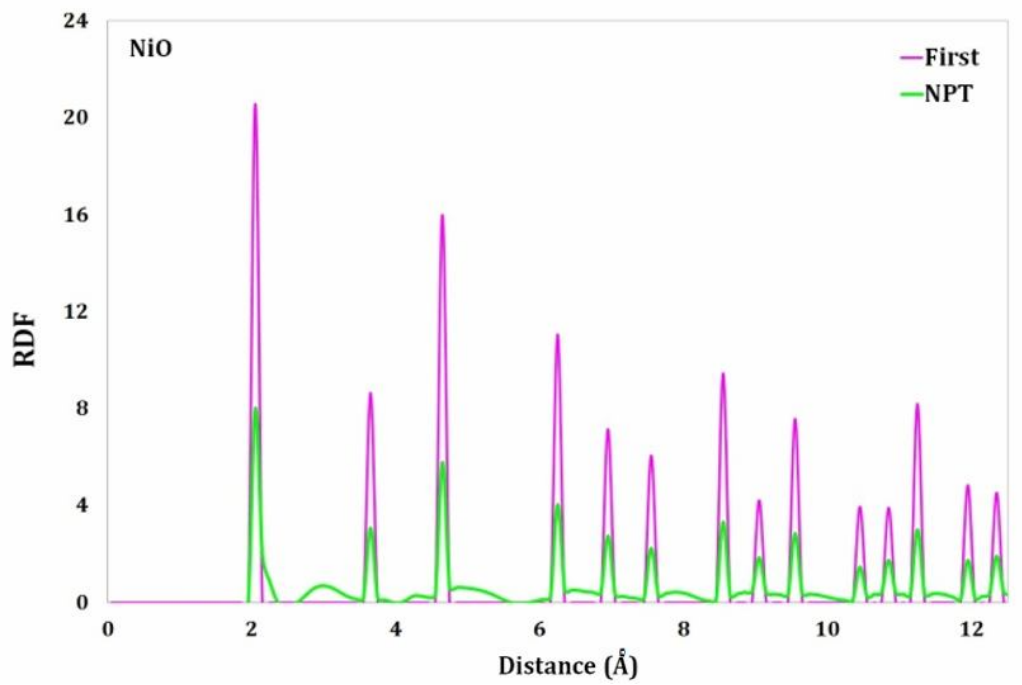

Fig. 3. The pair correlation function calculated for Ni-O before and after simulation.

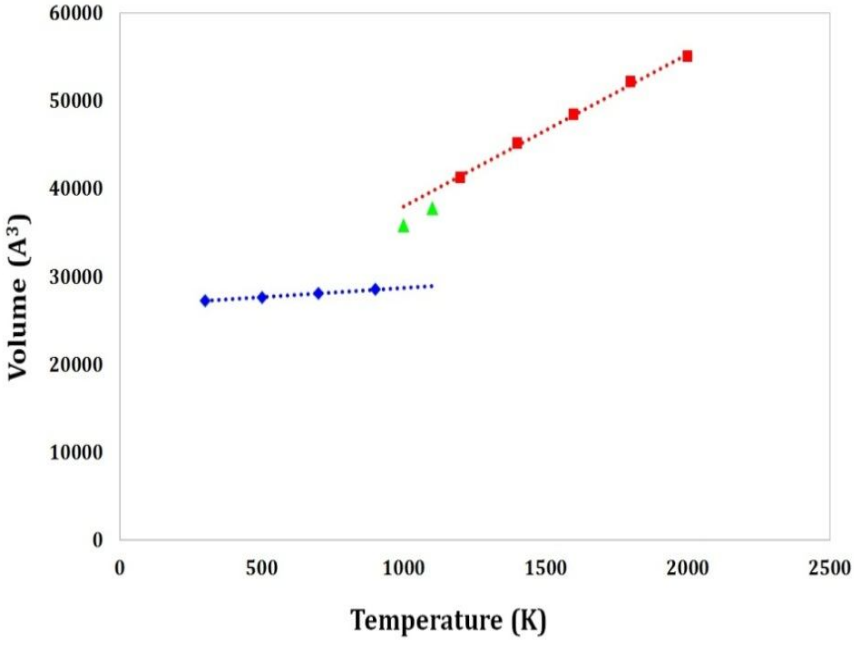

Fig. 4. Changes in the volume of the simulation box by increasing the temperature.

indicate that the system is in solid state. Also, since the RDF diagram was drown based on 100 frames of the present structure in the different times, low fluctuations are expected for the atoms in solid structures. In the other word, peak intensity is less compared to before the simulation.

Al/NiO Thermite Reaction

To gain further understanding of the phase changing processes and reaction occurring temperature, the simulations were conducted and Al/NiO thermite system with varying temperatures (*i.e.,* 300 K, 400 K, 500 K, 600 K, 700 K and 900 K) were observed. In this regard, a MD simulation with NPT ensemble was performed in the temperature range of 200-300 K with a time step of 1 fs within a period of 100 ps. It should be mentioned that the simulation box reached equilibrium through NVT ensemble and 10 ps prior to this step. As the energy and volume changes frequently occur in the reaction temperature, these two parameters were used to obtain the reaction temperature.

According to Fig. 4, the volume of the simulation box changes by increasing the temperature. As the results suggest, the simulation box changes are not high for the temperatures below 900 K; however, these changes increase with a constant slope. Since the melting point of aluminum is 933 K, the aluminum structure starts to melt at temperatures higher than 900 K, and it causes a rapid change in the system at 1000 K. This value is not necessarily the reaction temperature. The results also show that for the temperatures higher than 1200 K, changes in the volume of the simulation box have a complete linear trend in temperature increase when the system is in its equilibrium state. Therefore, phase changes and/or reaction occurred within the range of 900-1200 K, and since 900-1000 K range is related to the melting of aluminum the reaction occurred within the range of 1100-1200 K.

The potential energy (PE) changes in the system resulted from simulation is displayed in Fig. 5. As the results show, the PE of simulation box increases with a completely linear trend through an increase in the temperature. In this sense, the results indicate that the PE changes do not follow the previous linear trend for the temperatures higher than 900 K. As the melting point of aluminum is 993 K, this trend is expected for the temperatures higher than 900 K. The simulation results prove that for the temperatures higher than 1200 K, the trend of PE changing, based on temperature, is a decreasing trend with a constant slope. Therefore, these results demonstrate that the increasing trend of PE shifts to a decreasing trend by increasing the temperature with a constant slope. That is, there must be a reaction occurring in between. Therefore, this reaction occurs at the temperature range of 1100-1200 K. So, if we draw lines between the energy points before 1100 K and the temperatures higher than 1200 K, the intersection of these lines will be located approximately at 1141 K, that is, the reaction temperature. The reaction temperature of experimental results offered in this case is 1148.8 K [48], showing a good agreement with the results of this study.

The MD simulation using NVE ensemble was performed at five different temperatures, including 500, 900, 1100, 1200 and 1400 K with a time step of 1 fs in a period of 300 ps. It should be noted that the box d reached a thermal equilibrium in 10 ps with NVT ensemble prior to performing the simulation.

In Fig. 6, the temperature diagram of the simulation box is displayed as a function of time. As the results show, the temperature of the simulation box increases with time, that if it reaches a desirable temperature, a significant change in the reaction occurs. This will cause a rapid temperature rise, which will increase with a soft slope to reach the thermal equilibrium.

The closer the initial equilibrium temperature is to the thermite reactions occurring temperature, the increasing temperature has less time.

Moreover, the results show no sharp increase in temperature at 500 K, indicating that the thermite reactions occur above this temperature.

Since the reaction temperature is 1141 K, to deeply investigate the present thermite reaction process, the simulation box will be carefully studied at 1200 K before and after the MD simulation at NVE ensemble. In this case, Fig. 7 shows snapshots of the MD simulation for the initial temperature of 1200 K. As the MD simulation starts, the temperature of the atoms inside the box reaches an equilibrium at 1200 K, in which the atom movements are very high and the atoms lose their molecular structures with the time evolution and thus approach to each other.

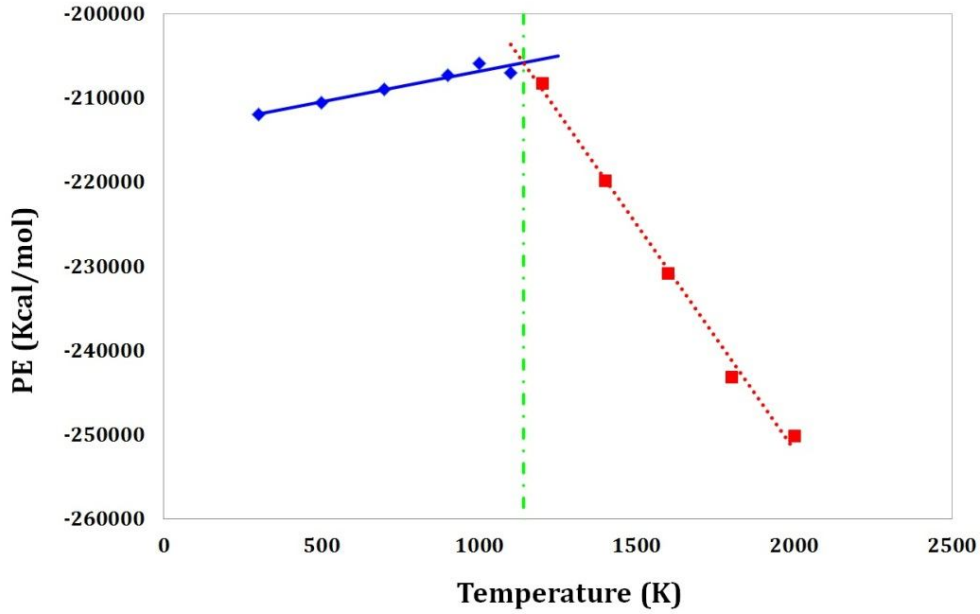

Fig. 5. Variation of potential energy (kcal mol^{-1}) with temperature for the present thermite reaction.

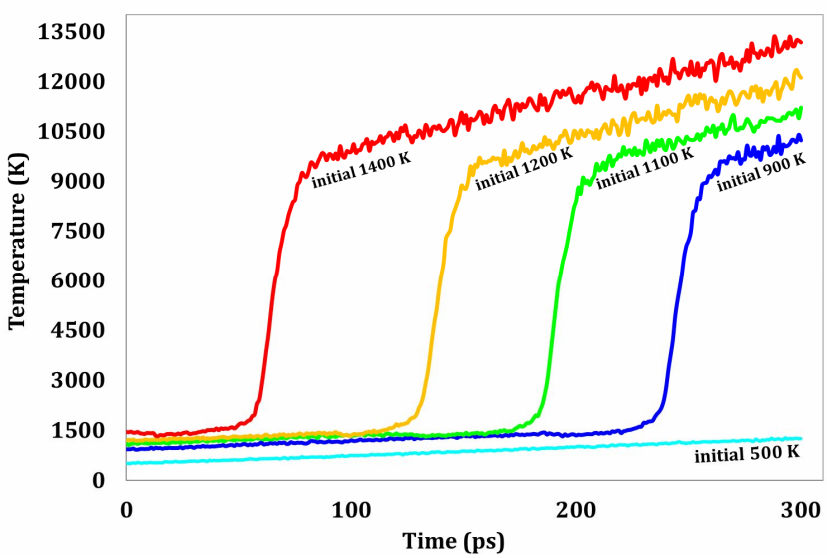

Fig. 6. Temperature profiles predicted for the Al/NiO thermite system with different initial temperatures.

When time approaches to 100 ps, the aluminum atoms come in contact with the NiO structure. Since there is a strong attraction between Al and O atoms, a few O atoms exit from the NiO structure and come in contact with Al surface; this is the beginning point of the collapse of the NiO structure. When the reaction time is greater than 100 ps and reaches to 200 ps, almost all oxygen atoms of the NiO structure diffuse between the Al atoms and the AlO structure starts to take shape as well. The simulation box does not obviously change with time while oxygen and

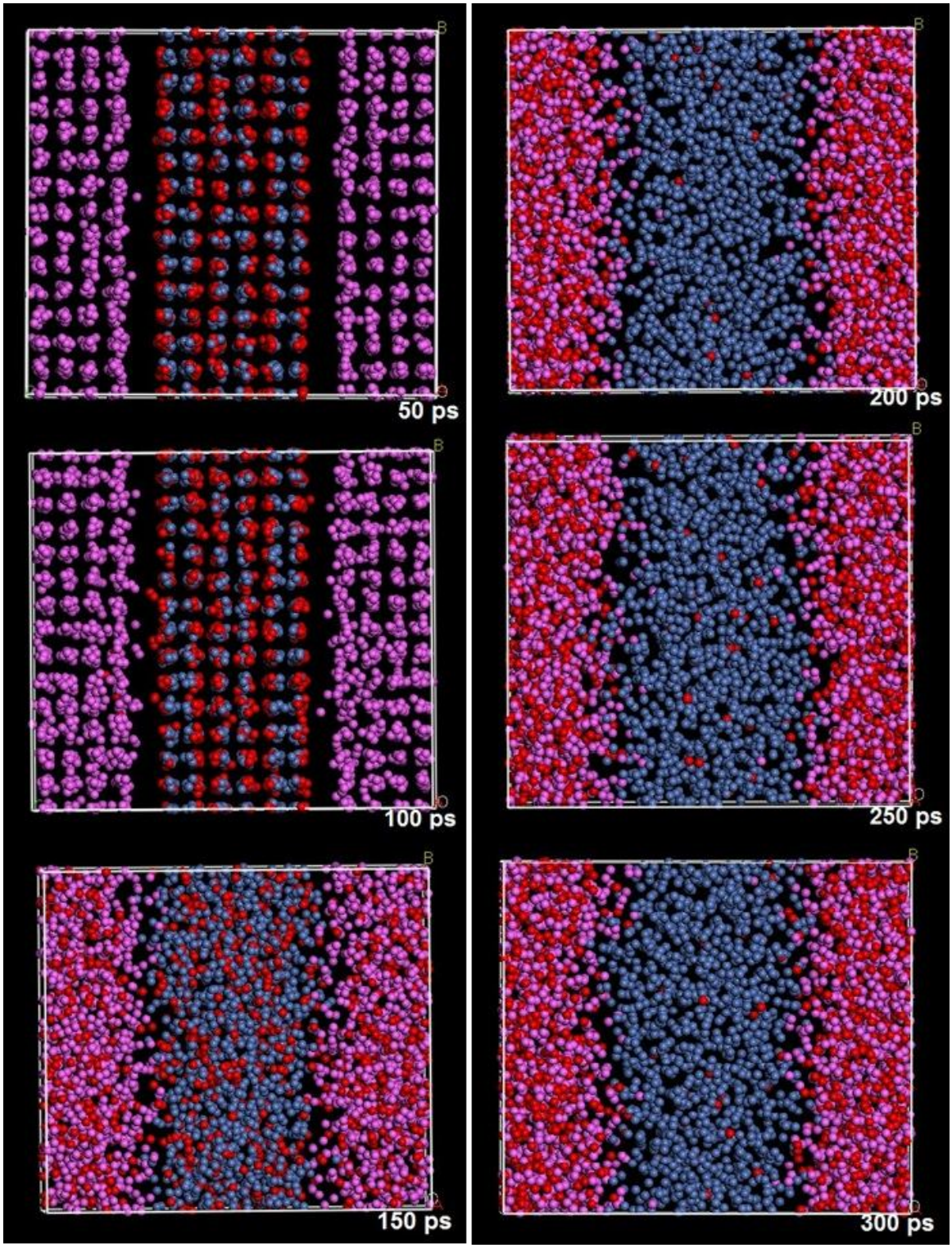

Fig. 7. Snapshots of the MD simulation for the initial temperature of 1200 (50 to 300 ps).

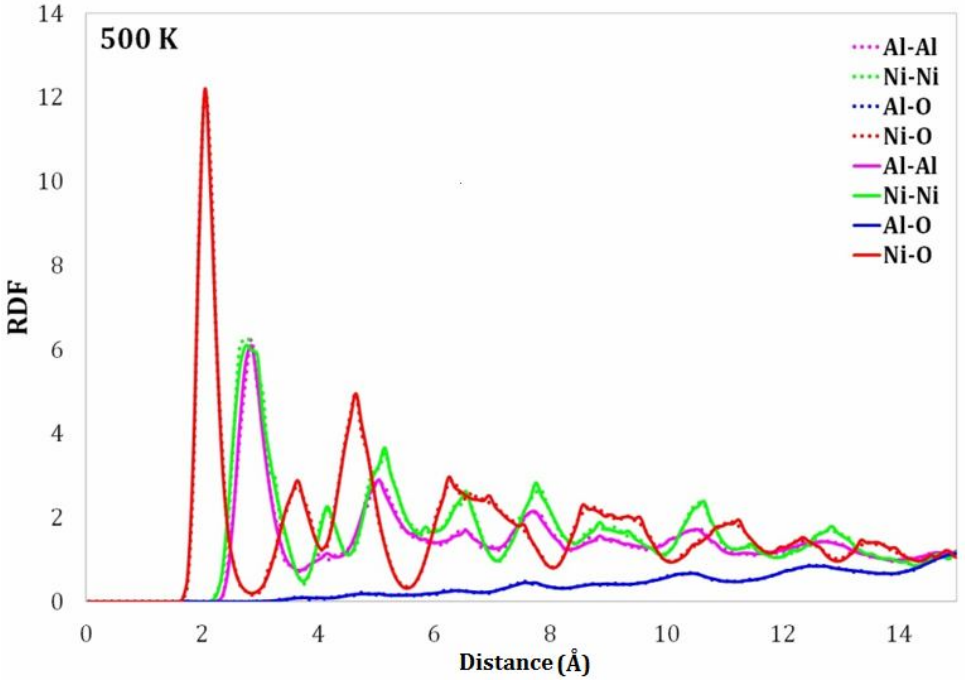

Fig. 8. The pair correlation function calculated for Ni-O, Ni-Ni, Al-O, and Al-Al at 500 K.

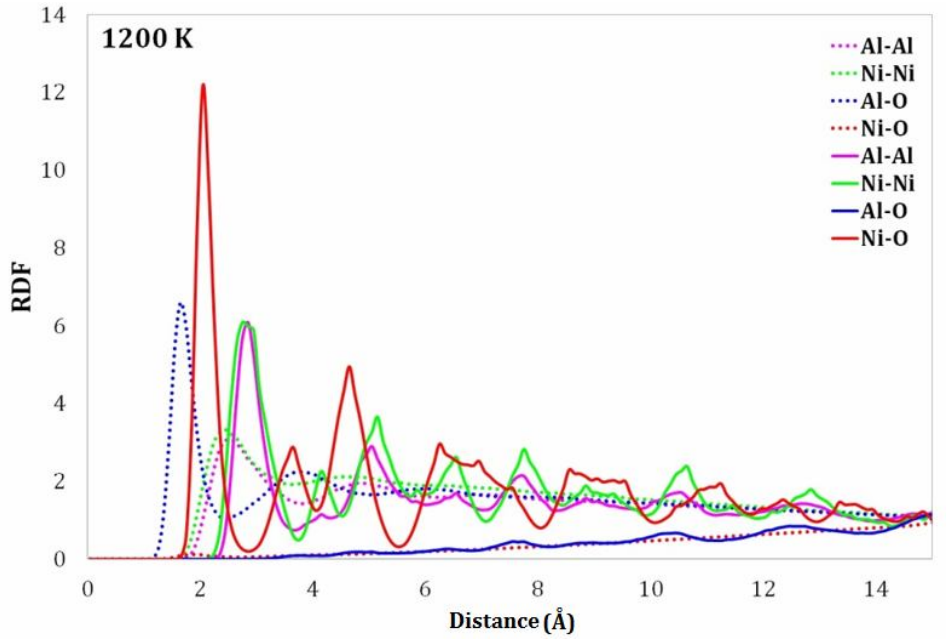

Fig. 9. The pair correlation function calculated for the Ni-O, Ni-Ni, Al-O, and Al-Al bonds before and after the simulation at 1200 K.

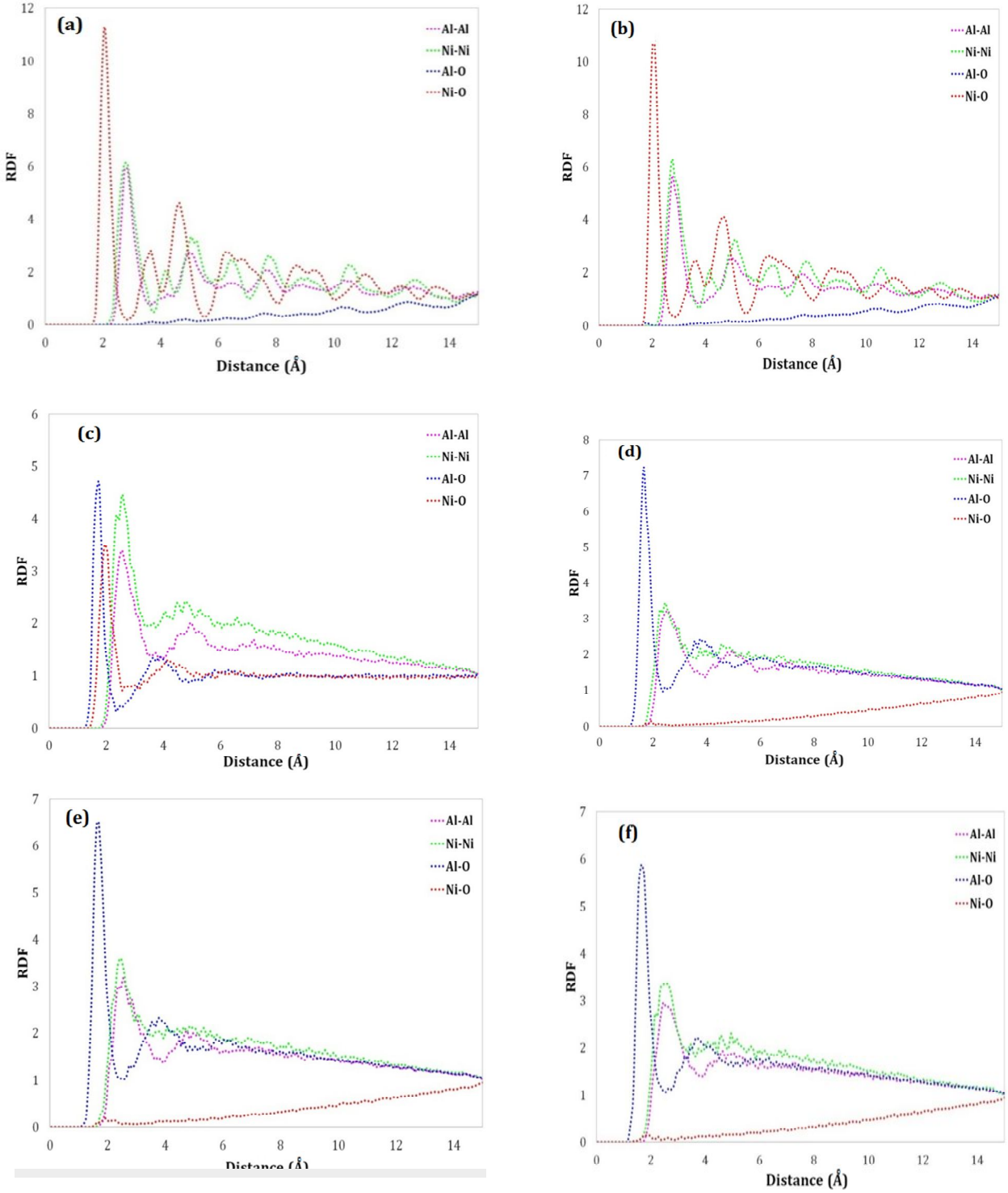

Fig. 10. The pair correlation function calculated for the Ni-O, Ni-Ni, Al-O, and Al-Al bonds at different simulation times (a) 50, (b) 100, (c) 150, (d) 200, (e) 250 and (f) 300 ps.

aluminum atoms are making the best structure of AlO and Ni atoms move toward a pure nickel metal structure. RDF analysis was used for a more accurate study of thermal reaction in this case. In Fig. 8, the results related to RDF at 500 K are displayed for Ni-O, Ni-Ni, Al-O, and Al-Al atom pairs. In this figure, the solid lines show the RDF data before the MD simulation and dotted lines are attributed to the RDF data after 300 ps of MD simulation.

The RDF diagram related to the Al/NiO system of Ni-O, Ni-Ni, Al-O, and Al-Al bonds at 1200 K before and after the MD simulation through NVE ensemble is displayed in Fig. 9.

The solid lines are attributed to the state before the simulation while the dotted lines are related to the state after the simulation. As the results show, the first and highest peaks before the simulation belong to Ni-O bond while Al-O has no link with each other. On the other hand, the RDF results obtained after the simulation show that the first and the highest peaks belong to Al-O bond. The red line in this diagram indicates the presence of Ni atoms along with O atoms. As can be seen, this red dotted line moves toward 1 with a low slope, suggesting a great distance between Ni and O atoms in the molecular structure of the simulation box at 1200 K. Therefore, we can claim that the NiO structure has been destroyed. The first and sharp peak belongs to the Ni-O bond located at 2.05 angstrom and the Ni-Ni and Al-Al peaks are set at 2.75 and 2.85 angstrom, respectively. As observed in Fig. 9, the Ni-Ni bond distance has shifted toward the lower value after the simulation, indicating that Ni atoms approach to each other to form a pure nickel metal.

Also, from Fig. 9 we concluded that after simulation, the Al-O peak were observed and indicate that the aluminum oxide is being formed. To have a more precise investigation of the thermal reaction process at 1200 K, RDF analysis was performed in different times. The results related to RDF obtained from the MD simulation through NVE ensemble for Ni-O, Ni-Ni, Al-O, Al-Al atom pairs at different times are displayed in Fig. 10.

The results show that after 50 ps, the first and highest peak of RDF diagram still belongs to Ni-O bond, and these diagrams are similar to the state before the simulation. However, Ni atoms approach to each other with time and the intensity of the peak related to this bond is increased. As Ni atoms approach to each other, O atoms exit the NiO structure and diffuse into the Al structure. Until 100 ps, no peaks are observed for the Ni-O bond. However, the first peak related to the Al-O bond is observed after 150 ps of the simulation, which indicates the formation of this bond. Furthermore, it shows that the intensity of RDF diagram related to Ni-O decreases as well. Therefore, at this time aluminum oxide and nickel oxide exist simultaneously in the simulation box. The results suggest that the oxygen atoms in nickel oxide structure migrate into the aluminum metal to form aluminum oxide, which means that our simulation successfully reproduces the thermite reaction in the Al/NiO system consisting initially of thin NiO and aluminum layers. For a deeper understanding, RDF diagram related to Al-O and Ni-O at different times are compared to each other. The results obtained for Al-O bond in Fig. 11 show that the tendency of O atoms to be placed near Al atoms increases with time so that the structure can reach an equilibrium and aluminum oxide can be formed as such.

Figurre 12 displays the RDF diagram for Ni-O bond for 1200 K at different times. The comparison of RDF diagrams shows that the crystal structure of NiO collapses with time. In addition, the tendency of O atoms to be near Ni atoms decreases, whereas Ni atoms show more tendency toward each other and this trend continues until the nickel metal structure is formed and the equilibrium is reached.

Figure 13 shows the RDF diagram related to the Al-O bond at different temperatures. The comparison of the RDF diagrams suggests that the crystal structure of NiO collapses by increasing temperature, whereas the tendency of O atoms to be near Al atoms increases. Therefore, no Al-O bond is formed at 500 K because no characteristic peak is observed in RDF diagram. For the temperatures higher than 900 K, the Al-O bond is formed in the simulation box gradually, and more oxygen atoms formed Al-O bonds by increasing the temperature. Difference in the height of the peaks is observed at lower temperatures due to the fact that some oxygen atoms are located at the NiO structure.

Mean square displacement (MSD) analysis can be used for analyzing the movement and permeation of atoms in the simulation box. Einstein showed that the mean square of the distance travelled by the particle following a random motion is proportional to the time elapsed [49]. The MSD is defined as the following Eq.

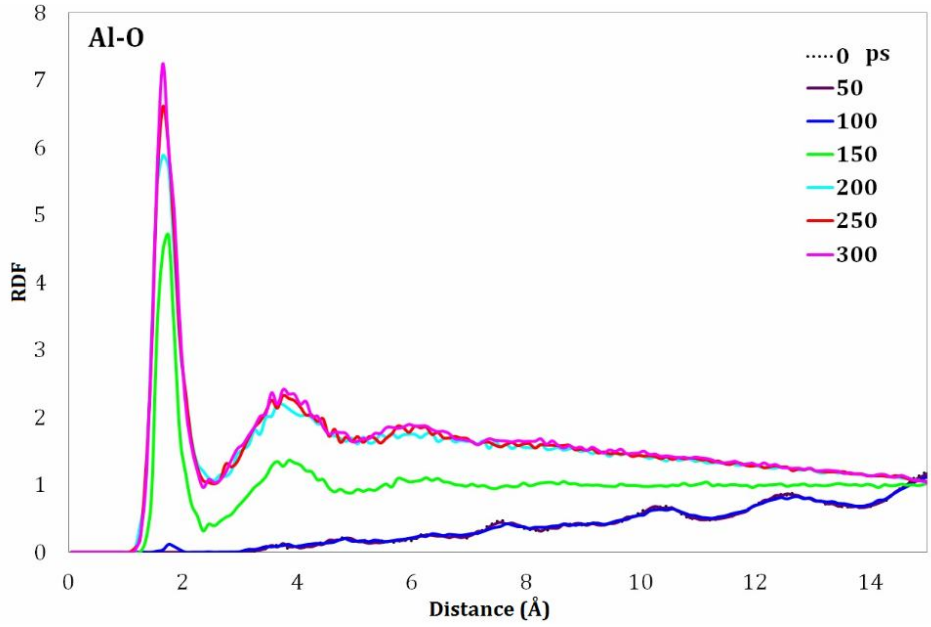

Fig. 11. The pair correlation function calculated for Al-O at different simulation times.

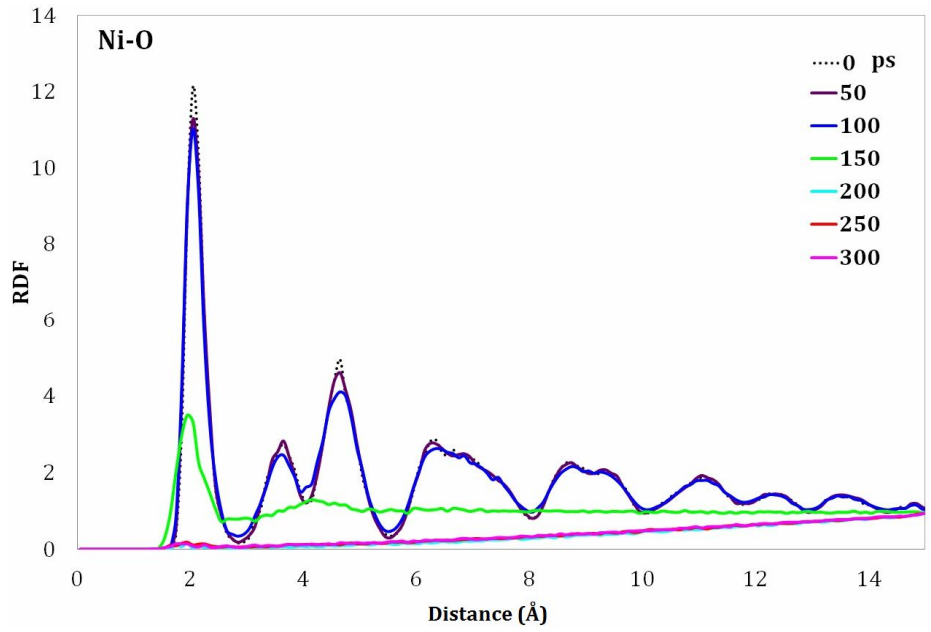

Fig. 12. The pair correlation function calculated for Ni-O at different simulation times.

$$MSD = \left\langle \left| \vec{r}(t) - \vec{r}(0) \right|^4 \right\rangle \quad (4)$$

where r(t) and r(0) represent the position vector of the center of the mass of compound i at initial and at time t. The average <…> designates a time-average over t. If the system is solid, the MSD saturates to a finite value while if

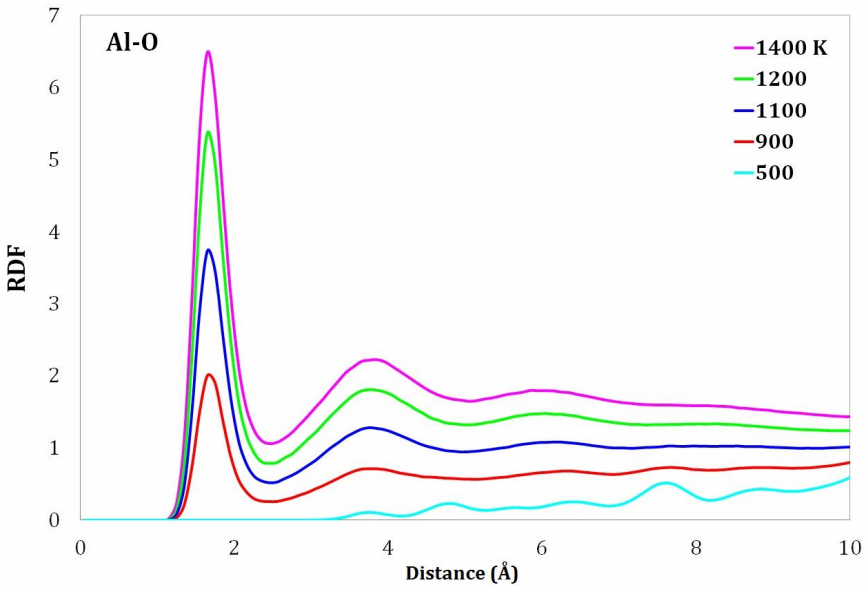

Fig. 13. The pair correlation function calculated for Al-O at different temperatures.

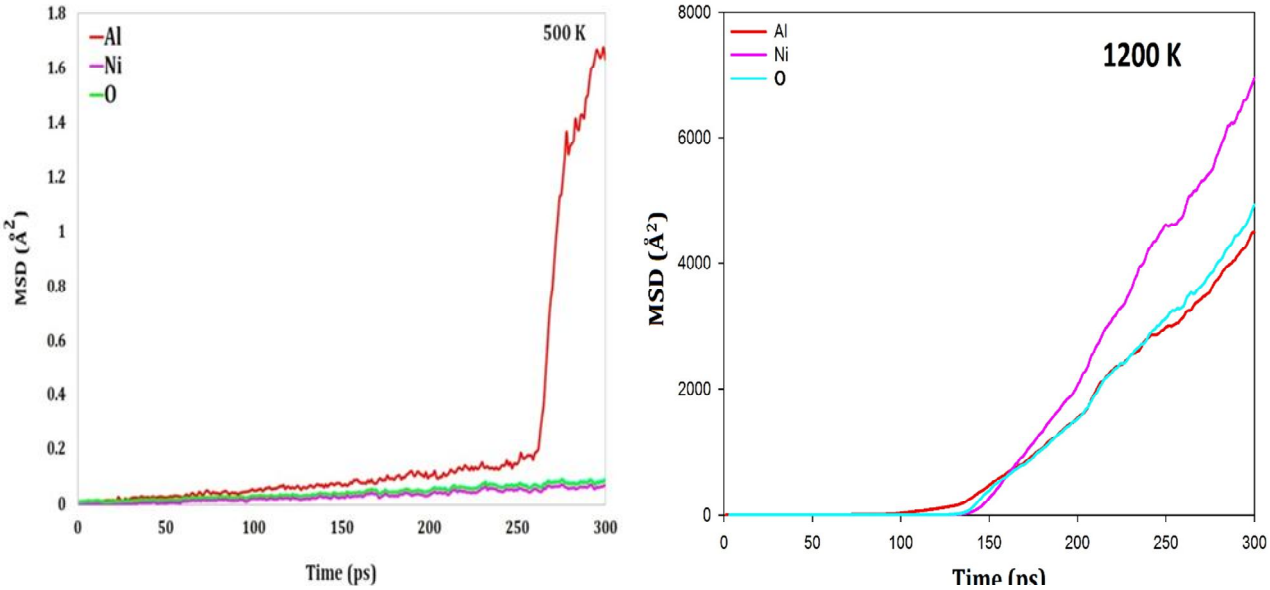

Fig. 14. The MSD plot of Al, Ni, and O atoms at 500 and 1200 K.

the system is liquid, the MSD linearly grows with time.

Figure 14 shows the MSD related to oxygen, aluminum, and nickel atoms at 500 and 1200 K. The figure at 500 K shows that the displacement of all atoms is close to zero except very low value for aluminum atom at the time step higher than 250 ps (consider the MSD scale axis at the 500

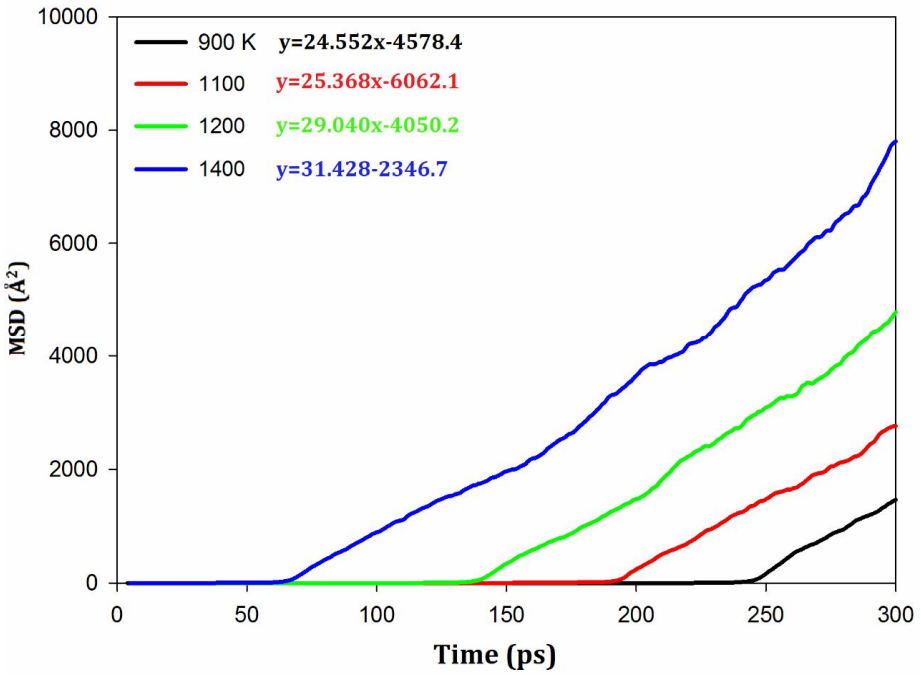

Fig. 15. The MSD plot change as a function of temperature.

Table 1. Self-diffusion Coefficients of Oxygen Atom at Various Temperatures

T (K)	D (10^{-8} m^2 s^{-1})
900	4.09
1100	4.23
1200	4.84
1400	5.24

and 1200 K). The results at 1200 K suggest that the MSD for Ni is higher than O and Al atmos. Since at the time step higher than 150 ps and 1200 K the thermite reaction occurs, Al and O atoms get close to each other to form the Al-O bond, and consequently the displacement decreases .

The MSD contains information on self-diffusion coefficient, D:

$$D = \lim_{t\to\infty}\left(\frac{MSD}{6t}\right) \quad (5)$$

The importance of this relation is that it relates the macroscopic transport coefficient D to the microscopic information on the MSD of molecular motion.

The self-diffusion coefficients of oxygen atom at

various temperatures were obtained from the slope of MSD plots (see Fig. 15); the results are summarized in Table 1. This figure shows that as the initial temperature increases, the effective time within which the thermite reaction occurs decreases. As shown in Table 1, the self-diffusion coefficient increases as the temperature increases, because the diffusion coefficient is the measure of the mobility of molecules.

CONCLUSIONS

The MD simulation was employed to investigate the behavior of the Al/NiO thermite reaction. Theoretically, the MD results show that 1142 K as a reaction temperature is in good agreement with the experimental 1148.8 K value. The RDF and MSD analyses were used to investigate the reaction mechanism and also the process of the broken/formed bonds. The RDF results show that no reaction occurs at 500 K, whereas at 1200 K the reaction was completely performed. Finally, the findings of the study indicate that as temperature increases, diffusion coefficient significantly increases as well.

REFERENCES

[1] Zhao, N.; He, C.; Liu, J.; Gong, H.; An, T.; Xu, H.; Zhao, F.; Hu, R.; Ma, H.; Zhang, J., Dependence of catalytic properties of Al/Fe_2O_3 thermites on morphology of Fe_2O_3 particles in combustion reactions., *J. Solid State Chem.* **2014**, *219*, 67-73, DOI: 10.1016/j.jssc.2014.06.039.

[2] Zhang, D.; Li, X., Fabrication and kinetics study of Nano-Al/NiO thermite film by electrophoretic deposition., *J. Phys. Chem. A.* **2015**, *119*, 4688-4694, DOI: 10.1021/jp5129113.

[3] Nguyen, N. H.; Hu, A.; Persic, J.; Wen, J. Z., Molecular dynamics simulation of energetic aluminum/palladium core-shell nanoparticles., *Chem. Phys. Lett.* **2011**, *503*, 112-117, DOI: 10.1016/ j.cplett.2010.12.074.

[4] Levchenko, E. V.; Evteev, A. V.; Riley, D. P.; Belova, I. V.; Murch, G. E., Molecular dynamics simulation of the alloying reaction in Al-coated Ni nanoparticle., *Comput. Mater. Sci.* **2010**, *47*, 712-720, DOI: 10.1016/j.commatsci.2009.10.014.

[5] Prathab, B.; Subramanian, V.; Aminabhavi, T. M., Molecular dynamics simulations to investigate polymer-polymer and polymer-metal oxide interactions. *Polymer*, **2007**, *48*, 409-416, DOI: 10.1016/j.polymer.2006.11.014.

[6] Coffey, K. R.; Dein, E.; Hugus, D.; Sheridan, E., In; Google Patents: 2013.

[7] Iordachescu, M.; Iordachescu, D.; Scutelnicu, E.; Ruiz-Hervias, J.; Valiente, A.; Caballero, L., Influence of heating source position and dilution rate in achieving overmatched dissimilar welded joints. *Sci. Technol. Welding & Joining.* **2010**, *15*, 378-385, DOI: 10.1179/136217110X12693513264259.

[8] Chen, Y.; Lawrence, F. V.; Barkan, C. P.; Dantzig, J., Heat transfer modelling of rail thermite welding. *Proceedings of the Institution of Mechanical Engineers, Part F: Journal of Rail and Rapid Transit.* **2006**, *220*, 207-217, DOI: 10.1243/09544097F01505.

[9] Yi, W.; Wei, J.; Lixin, L.; Hongying, L.; Yaqing, L.; Fengsheng, L., Thermal reactivity of nanostructure Al 0.8Mg0.2 alloy powder used in thermites. *Rare Metal Mate. Engin.* **2012**, *41*, 9-13, DOI: 10.1016/S1875-5372(12)60021-6.

[10] Varma, A.; Lebrat, J. P., Combustion synthesis of advanced materials. *Korean J. Chem. Engin.* **1992**, *47*, 2179-2194, DOI: 10.1007/BF02705444.

[11] Martirosyan, K. S., Nanoenergetic Gas-Generators: principles and applications. *J. Mater. Chem.* **2011**, *21*, 9400-9405, DOI: 10.1039/C1JM11300C.

[12] Wang, L. L.; Munir, Z. A.; Maximov, Y. M., Thermite reactions: their utilization in the synthesis and processing of materials. *J. Mater. Sci.,* **1993**, *28*, 3693-3708, DOI: 10.1007/bf00353167.

[13] Patil, K. C.; Aruna, S. T.; Ekambaram, S., Combustion synthesis. *Current Opinion in Solid State and Materials Science.* **1997**, *2*, 158-165, DOI: 10.1016/S1359-0286(97)80060-5.

[14] Martirosyan, K. S.; Hobosyan, M.; Lyshevski, S. E., Enabling nanoenergetic materials with integrated microelectronics and MEMS platforms. In Nanotechnology (IEEE-NANO), 2012 12th IEEE Conference on, 2012; IEEE: 2012; pp. 1-5.

[15] Kuntz, J. D.; Cervantes, O. G.; Gash, A. E.; Munir, Z.

A., Tantalum-tungsten oxide thermite composites prepared by sol-gel synthesis and spark plasma sintering. *Combus Flame.* **2010**, *157*, 1566-1571, DOI: 10.1016/j.combustflame.2010.01.005.

[16] Staley, C.; Morris, C.; Thiruvengadathan, R.; Apperson, S.; Gangopadhyay, K.; Gangopadhyay, S., Silicon-based bridge wire micro-chip initiators for bismuth oxide-aluminum nanothermite. *J. Micromechanics and Microengin.* **2011**, *21*, 115015, DOI: 10.1088/0960-1317/21/11/115015.

[17] Wang, J.; Hu, A.; Persic, J.; Wen, J. Z.; Zhou, Y. N., Thermal stability and reaction properties of passivated Al/CuO nano-thermite. *J. Phys. Chem. Solids.* **2011**, *72*, 620-625, DOI: 10.1016/j.jpcs.2011.02.006.

[18] Zhu, P.; Shen, R.; Ye, Y.; Zhou, X.; Hu, Y., Energetic igniters realized by integrating Al/CuO reactive multilayer films with Cr films. *J. Appl. Phys.* **2011**, *110*, 074513, DOI: 10.1063/1.3646489.

[19] Higa, K. T., Energetic nanocomposite lead-free electric primers. *J. Propulsion and Power.* **2007**, *23*, 722-727, DOI: 10.2514/1.25354.

[20] Wang, L. L.; Munir, Z. A.; Maximov, Y. M., Thermite reactions: their utilization in the synthesis and processing of materials. *J. Mater. Sci.* **1993**, *28*, 3693-3708, DOI: 10.1007/bf00353167.

[21] Dreizin, E. L., Metal-based reactive nanomaterials. *Progress in Energy and Combustion Science.* **2009**, *35*, 141-167, DOI:10.1016/j.pecs.2008.09.001.

[22] Goldschmidt, Verfahren zur Herstellung von Metallen oder Metalloiden oder Legierungen derselben" (Process for the production of metals or metalloids or alloys of the same), Deutsche Reichs Patent no. 96317 (13 March 1895).

[23] Sullivan, K. T., Ignition, Combustion and Tuning of Nanocomposite Thermites. (2010). at <drum.lib.umd.edu/handle/1903/11119>.

[24] Cheng, J. L.; Hng, H. H.; Lee, Y. W.; Du, S. W.; Thadhani, N. N., Kinetic study of thermal- and impact-initiated reactions in Al-Fe_2O_3 nanothermite. Combust. *Flame.*, **2010**, *157*, 2241-2249, DOI: 10.1016/j.combustflame.2010.07.012.

[25] Zhu, Z. Y.; Ma, B.; Tang, C. -M.; Cheng, X. L., Molecular dynamic simulation of thermite reaction of Al nanosphere/Fe_2O_3 nanotube. *Phys. Lett. A.,* **2016**, *380*, 194-199, DOI: 10.1016/j.physleta.2015.09.041.

[26] Durães, L.; Costa, B. F. O.; Santos, R.; Correia, A.; Campos, J.; Portugal, A., Fe_2O_3/aluminum thermite reaction intermediate and final products characterization. *Mater. Sci. Eng: A.,* **2007**, *465*, 199-210, DOI: 10.1016/j.msea.2007.03.063.

[27] Apperson, S.; Shende, R. V.; Subramanian, S.; Tappmeyer, D.; Gangopadhyay, S.; Chen, Z.; Gangopadhyay, K.; Redner, P.; Nicholich, S.; Kapoor, D., Generation of fast propagating combustion and shock waves with copper oxide/aluminum nanothermite composites. *Appl. Phys. Lett.,* 2007, *91*, 243109, DOI: 10.1063/1.2787972.

[28] [28] Séverac, F.; Alphonse, P.; Estève, A.; Bancaud, A.; Rossi, C., High-Energy Al/CuO Nanocomposites Obtained by DNA-Directed Assembly. *Adv. Funct. Mater.,* **2012**, *22*, 323-329, DOI: 10.1002/ adfm.201100763.

[29] Kwon, J.; Ducéré, J. M.; Alphonse, P.; Bahrami, M.; Petrantoni, M.; Veyan, J. F.; Tenailleau, C.; Estève, A.; Rossi, C.; Chabal, Y. J., Interfacial chemistry in Al/CuO reactive nanomaterial and its role in exothermic reaction. *ACS Appl. Mater. & Interface.,* **2013**, *5*, 605-613, DOI: 10.1021/am3019405.

[30] Son, S. F.; Asay, B. W.; Foley, T. J.; Yetter, R. A.; Wu, M. H.; Risha, G. A., Combustion of nanoscale Al/MoO_3 thermite in microchannels. *J. Propul. Power.,* **2007**, *23*, 715-721, DOI: 10.2514/1.26090.

[31] Sun, J.; Pantoya, M. L.; Simon, S. L., Dependence of size and size distribution on reactivity of aluminum nanoparticles in reactions with oxygen and MoO_3. *Thermochim Acta.,* **2006**, *444*, 117-127, DOI: 10.1016/j.tca.2006.03.001.

[32] Sullivan, K. T.; Chiou, W. -A.; Fiore, R.; Zachariah, M. R., *In situ* microscopy of rapidly heated nano-Al and nano-Al/WO3 thermites. *Appl. Phys. Lett.,* **2010**, *97*, 133104, DOI: 10.1063/1.3490752.

[33] Puszynski, J. A.; Bulian, C. J.; Swiatkiewicz, J. J., Processing and ignition characteristics of aluminum-bismuth trioxide nanothermite system. *J. Propul. Power.,* **2007**, *23*, 698-706, DOI: 10.2514/1.24915.

[34] Wang, L.; Luss, D.; Martirosyan, K. S., The behavior of nanothermite reaction based on Bi_2O_3/Al. *J. Appl. Phys.* **2011**, *110*, 074311, DOI: 10.1063/1.3650262.

[35] Rossi, C.; Zhang, K.; Esteve, D.; Alphonse, P.; Tailhades, P.; Vahlas, C., Nanoenergetic materials for MEMS: *A Review. J. Microelectromech. Syst.,* **2007**, *16*, 919-931, DOI: 10.1109/JMEMS.2007.893519.

[36] Zhang, K.; Rossi, C.; Alphonse, P.; Tenailleau, C.; Cayez, S.; Chane-Ching, J. -Y., Integrating Al with NiO nano honeycomb to realize an energetic material on silicon substrate. *Appl. Phys. A.,* **2009**, *94*, 957-962, DOI: 10.1007/s00339-008-4875-6.

[37] Wen, J. Z.; Ringuette, S.; Bohlouli-Zanjani, G.; Hu, A.; Nguyen, N. H.; Persic, J.; Petre, C. F.; Zhou, Y. N., Characterization of thermochemical properties of Al nanoparticle and NiO nanowire composites. *Nanoscale Res. Lett.,* **2013**, *8*, 1-9, DOI: 10.1186/1556-276x-8-184.

[38] Wang, Y.; Song, X. L.; Jiang, W.; Deng, G. D.; Guo, X. D.; Liu, H. Y.; Li, F. S., Mechanism for thermite reactions of aluminum/iron-oxide nanocomposites based on residue analysis. *Trans. Nonferrous Met. Soc. China.,* **2014**, *24*, 263-270, DOI: 10.1016/S1003-6326(14)63056-9.

[39] Senftle, T.; Sungwook, H.; Islam, M.; Kylasa, S.; Zheng, Y.; Kyung, Y. S.; Junkermeier, C.; Engel-Herbert, R. J.; Janik, M.; Metin Aktulga, H.; Verstraelen, T.; Grama, A.; van Duin, A. C. T., The ReaxFF reactive forcefield: development, applications and future directions,. *npj Comput. Mater.,* **2016**, 2, 15011, DOI: 10.1038/npjcompumats.2015.11.

[40] Jin-Ping, Z.; Zhang, Y. Y.; Hui, L.; Jing-Xia, G.; Xin-Lu, C., Molecular dynamics investigation of thermite reaction behavior of nanostructured Al/SiO_2 system. *Acta Phys. Sin.,* **2014**, *63*, 086401, DOI: 10.7498/aps.63.086401.

[41] Assowe, O.; Politano, O.; Vignal, V.; Arnoux, P.; Diawara, B., A reactive force field molecular dynamics simulation study of corrosion of nickel, *Def. Diff. Forum.,* **2012**, *323-325*, 139-145, DOI: 10.4028/www.scientific.net/DDF.323-325.139.

[42] Tersoff, J., New empirical approach for the structure and energy of covalent systems. *Phys. Rev. B.,* **1988**, *37*, 6991-7000, DOI: 10.1103/ PhysRevB.37.6991.

[43] Brenner, D. W.; Empirical potential for hydrocarbons for use in simulating the chemical vapor deposition of diamond films. *Phys. Rev. B.,* **1990**, *42*, 9458-9471, DOI: 10.1103/PhysRevB.42.9458.

[44] Hong, S.; van Duin, A. C. T., Molecular dynamics simulations of the oxidation of aluminum nanoparticles using the ReaxFF reactive force field. *J. Phys. Chem. C.,* **2015**, *119*, 17876-17886, DOI: 10.1021/acs.jpcc.5b04650.

[45] Ostadhossein, A.; Kim, S. Y.; Cubuk, E. D.; Qi, Y.; van Duin, A. C. T., Atomic insight into the lithium storage and diffusion mechanism of SiO_2/Al_2O_3 electrodes of lithium ion batteries: ReaxFF reactive force field modeling. *J. Phys. Chem. A.* **2016**, *120*, 2114-2127, DOI: 10.1021/acs.jpca.5b11908.

[46] Shin, Y. K.; Kwak, H.; Zou, C.; Vasenkov, A. V.; van Duin, A. C., Development and validation of a ReaxFF reactive force field for Fe/Al/Ni alloys: Molecular dynamics study of elastic constants, diffusion, and segregation., *J. Phys. Chem. A.,* **2012**, *116*, 12163-12174, DOI: 10.1021/jp308507x.

[47] Sanz-Navarro, C. F.; Åstrand, P. -O.; Chen, D.; Rønning, M.; Duin, A. C. T. v.; Mueller, J. E.; Goddard Iii, W. A., Molecular dynamics simulations of carbon-supported Ni clusters using the reax reactive force field. *J. Phys. Chem. C.,* **2008**, 112, 12663-12668, DOI: 10.1021/jp711825a.

[48] Fathollahi, M., Thermal Characterizations and Kinetic Analysis of Nano- and Micron-Al/NiO Thermite. Propellants, Explosives, Pyrotechnics, In press.

[49] Ermak, D. L.; McCammon, J. A., Brownian dynamics with hydrodynamic interactions. *J. Chem. Phys.,* **1978**, *69*, 1352-1360, DOI: 10.1063/1.436761.